Research Article

Modeling of a brushless dc motor driven electric vehicle and its pid-fuzzy control with dSPACE

Ali BAHADIR[1]* , Ömer AYDOĞDU[2]

¹Istanbul Technical University, Faculty of Electricaland Electronic Engineering, Department of Electronics and Communication Engineering, Istanbul, 34467, Türkiye

²Konya Technical University, Faculty of Engineering and Natural Sciences, Department of Electrical and Electronics Engineering, Konya,42130, Türkiye

ARTICLE INFO

ABSTRACT

In this study, a high power (75 kW) original driver and control algorithm has been developed for an electric passenger vehicle whose features can be used practically. It has been observed that some problems occur in the operation of the developed control algorithms in traction systems operating at high power. In this study, the solution methods of these problems are included. Firstly, the simulation model of an electrical vehicle was obtained by determining the basic parameters for a passenger electric vehicle. Then a brushless DC motor and drive system was determined for the electric vehicle and an original 75 kW DC-AC Converter (Inverter) in accordance with automotive standards has been designed and tested for the Brushless DC motor. Also, in the design and implementation phase, PID and Fuzzy control-based vehicle control software was developed in MATLAB/Simulink environment on the purpose of rapid prototyping and loaded on the DS1401 dSPACE based control system. It has been seen that through rapid prototyping, the appropriate controller development cycle time for the vehicle drastically reduced, which significantly has reduced the research and development costs. In the vehicle control algorithm, speed information is used as a reference input and brake information is used as feedback. The control signal generated by the controller is converted into PWM pulses for each phase and applied to the IGBT driver. These PWM pulses were used to switch the six IGBT power components used in the three-phase full-bridge DC-AC converter. Driving performance at the design stage has been studied for cases of starting, speed, reversal and load failure. Simulation and experimental results demonstrated the effectiveness of the driver and drive control system that were originally developed. When the system response was examined, it was revealed that the fuzzy logic control algorithm presented much better results than the PI and then the PID control algorithm. Simulation results and application results were consistent with each other and the system performance was successfully tested. Many protection circuits have been designed and configured in the system, with the control algorithms developed according to the problems arising in the operation of high-power systems, hardware add-ons for the operation of the high power (75kW) power-train. Safety

*Corresponding author.
*E-mail address: bahadiral@itu.edu.tr; bahadir_ali@hotmail.com

This paper was recommended for publication in revised form by Regional Editor Fatih Akyol

and security infrastructures have been developed in both hardware and software for the appropriate certification in automotive standards.

INTRODUCTION

Today, all the world countries have focused on new technologies for reducing the environmental pollution caused by the increase in fuel fossil-derived energy consumption and reducing the oil-derived fuel dependence. In the direction of the efforts in this, especially in recent years, most automotive manufacturers have increased their research and development activities on electric vehicles. These efforts in automotive technology indicate that the studies that started with hybrid vehicles are almost completely moved to electric vehicles today [1-3].

It is seen that the priorities of automotive companies working on electric vehicles agree on two aspects. The first of these two important issues is energy planning and the other is energy efficiency.

Increasing the efficiency of electric motors and drivers, reducing their losses such as switching, transmission etc. and keeping energy consumption at the minimum level are among the most important issues. Moreover, it is very important to choose the correct control method of these motors and their drivers and to write the control algorithm well. These issues will lead to an increase in the distance traveled by the vehicle and a decrease in unit energy consumption per km. It is observed that automotive companies focus on these issues [4-7].

Automotive companies producing electric vehicles tended to use Brushless Direct Current (BLDC) motor, which has positive features such as high efficiency, high momentum, low volume, and weight structure. BLDC motor using high energy permanent magnets is rapidly becoming widespread in applications. Technological developments in motor design lead to the development of control methods and control algorithms of these motors. [7-10].

One of the key points of this issue is to determine the parameters of the vehicle to be designed as an electric vehicle such as weight, acceleration, and the slope it can climb. As a result of the determined parameters, vehicle modeling should be done and the power to move this vehicle should be identified. Then, according to the determined power, bus-bar voltage and current selection, electric motor type selection, motor driver topology, which is appropriate for this motor, then the design of the control unit that will control this system and the software should be realized.

In the simulations performed in this study, creating a more realistic vehicle model based on real vehicle parameters and obtaining the mathematical model of the BLDC motor used in the most accurate way are the important points of the study. Brushless DC motors, which are among special electric motors, have a trapezoidal back EMF waveform due to their magnetic design, and the current waveform is not sinusoidal. However, in some simulation studies given in the literature, the back EMF model is considered as sinusoidal and analyzes and simulations are made accordingly. However, Considering the back EMF model in a trapezoidal shape and making analysis and simulations accordingly is a more correct approach. While vector control method can be applied to brushless synchronous motors with sinusoidal current and voltage waveforms, vector control method cannot be applied to BLDC motor due to its structure [11]. Another important point for simulation is that in the numerical solutions of the motor model the calculation error is minimized. For this purpose, it is aimed to obtain an effective solution in the simulation model of BLDC motor using discrete-time controller.

Calculations made on the vehicle dynamic model showed that the nominal power of the vehicle should be 75kW. Motor selection and drive systems were designed accordingly. The original design of the power electronics driver circuit with a power of 75 kW was realized, and then the nominal voltage value of the accumulator group to be used due to the nominal bus-bar voltage of the electric vehicle was determined as 375V. The original 75 kW liquid-cooled, fully controlled three-phase DC-AC HIL converter set was used and loaded for tests.

The control algorithms were developed in MATLAB/Simulink environment and the control algorithms were uploaded to DS1401 dSPACE MicroAuto-Box used in the application. Here, the dSPACE infrastructure enables the development of the control algorithm by changing the parameters of the real-time system.

With the control software designed in MATLAB/Simulink environment, trigger pulses required to operate the switching components of the three-phase fully controlled bridge converter are generated. Hall-effect sensors were used to determine the BLDC motor rotor position. These Hall-effect sensor signals, phase current detection signal and speed command are applied as the inputs of the digital controller. Both current and speed PI, PID and Fuzzy logic controllers are designed in the MATLAB/Simulink environment. Testing of the real-time system has been successfully performed by loading the control algorithms into the dSPACE processor. All of these operations are based on

the latest literature studies and new technological developments on these issues.

Many methods have been applied for Fuzzy Logic Control of BLDC motor such as Fuzzy logic with self-tuning, Fuzzy Sliding Mode, Fuzzy logic with self-tuning, Fuzzy Sliding Mode Control (FSMC) etc.

Bin Wu [12] used an Fuzzy logic control with self-tuning method of BLDC motor; it combines the ANN and PSO methods to produce the Membership Function parameters of Fuzzy Logic. The resulting steady state error is very low compared to the PI and FLC methods. Premkumar, K. and Manikandan [13] used an Bat Algorithm Optimized Fuzzy Proportional Derivative method; BLDC motor speed control system design with simulation using MATLAB/ Simulink and Sim power system tools. The optimization results are then compared with several other methods to obtain the best control result. The proposed control system provides a drastic improvement in measuring performance and better noise compensation than other methods. Chico A.H.B etc. [14] used an Fuzzy PI Controller method; Constant speed and variable speed tests of four switch converter designs were performed for BLDC motor drives using Fuzzy control with PI control parameters. Agrawal, S. And Vivek S. [15] used an PSO-Fuzzy method of BLDC motor; The combination of PSO and Fuzzy can provide better performance compared to conventional / PI methods. Wang, H., P. etc. [16] Fuzzy adaptive PID Controller methods; The proposed control method can increase the effectiveness of BLDC motor, where this control can be a solution to several problems that are difficult to overcome with conventional methods. Davoudkhani, I.F. and Akbari, M. [17] Interval Type-2 Fuzzy Logic based PID Controller (IT2FLPIDC) methods of BLDC motor; IT2FLPIDC can solve problems of uncertainty and variations in working conditions. The test results of the proposed system were then compared with the PID and Type-1 methods, and the results showed that IT2FLPIDC provided superior performance and response compared to the two methods. Wang, Z.S. etc. [18] Variable Universe Fuzzy Adaptive PID Control System of BLDC motor; The design of the BLDC motor speed control system uses PID adaptive universal variable control. The test is carried out on MATLAB / Simulink with a series of double closed-loop speed regulations which then performs performance analysis. The PSO algorithm is then applied to identify the optimal scaling factor.

These improved control algorithms have not been experienced in high power traction systems and the control software has not been redesigned to solve power electronics problems. Solution suggestions for the problems in high power applications are given. Hardware and software developments have been made to solve the power electronics problems that occur when the vehicle's BLDC motor slows down and brakes. The developed system was run on the HIL system and passenger car. It has been observed that the BLDC motor causes damage to the Back-EMF power

modules that occur when the vehicle slows down, stops and the vehicle goes down the ramp. For this, protection diodes are added to the power semiconductors, snubber capacitors are added to the inputs of the power semiconductors, DC-Bus capacitors are connected to the DC-Bus with the appropriate bus-bar, and a resistor that can be controlled via another power semiconductor is connected to the DC-Bus. DC-Bus and currents drawn from each phase are measured with current sensors. The control software switches the DC-Bus power semiconductor on when the measurement of the current sensors reaches the critical limit for the circuit. In addition, in case the BLDC motor is slowed down or stopped, the power semiconductor on the DC-Bus is transmitted during this time, and the back-EMF is converted into heat over the resistor.

MODELLING OF ELECTRIC VEHICLE AND BLDC MOTOR DRIVE SYSTEM

The general model of the electric vehicle was realized in MATLAB Simulink program according to the basic vehicle parameters. Major forces acting on a vehicle are; aerodynamic drag force, rolling friction resistance force and slope resistance force. If the vehicle is accelerating, the acceleration force will come in addition to these forces. In Figure 1 below, force components affecting the vehicle are given. Also, vehicle parameters considered in the study are shown in Table 1 below. Simulink model of the vehicle is shown in Figure 2. When he controls signal is at its maximum value, the motor average voltage should be selected as the bus-bar voltage. The internal structure of the vehicle model is shown in Figure 3.

BLDC motor model is similar to a conventional Brushed DC motor model under certain assumptions. BLDC motor's effective torque and speed control are based on moment and EMF equations similar to direct current motor equations. The BLDC motor state space model is a fourth-order equation that includes motor speed and phase currents. Output are expressed in terms of state variables and source voltage. Thus, a set of differential equations has been obtained for each position depending on the rotor position by using the general circuit analysis theory.
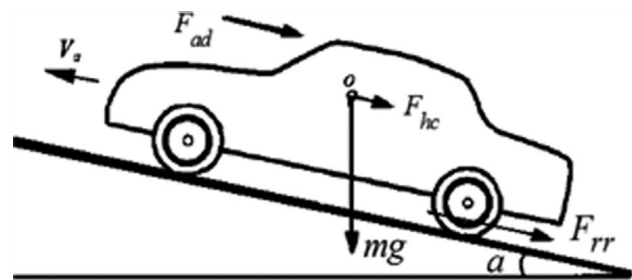

Figure 1. Force components acting on the vehicle.

As required by the 120 degrees' transmission condition of the brushless direct current motor, while two of the three phases are in transmission, current flows from all three phases in the commutation range.

Table 1. Vehicle Parameters

Parameter	Value	Unit	Description
m	1600	kg	Vehicle mass
w	4	*	Number of wheel
Jt	1,140	kg.m^2	Moment of inertia of a wheel
Bt	0,010	Nm.s/rad	A tire's viscous friction
Crr	0,010	*	Tire rolling resistance
Ro	1,293	kg/m^3	Air density
Cx	0,120	*	Aerodynamic coefficient
A	1	m^2	Vehicle cross section
Rt	0,265	m	Tire effective radius
α	0,2967	rad	Slope
g	9,810	m/s^2	Gravitational acceleration
u	1	*	Gear Rotation Ratio
Va	-	-	Velocity
mg	-	-	The force of gravity
Fad	-	-	Wind resistance
Fhc	-	-	The reverse force due to the slope.

BLDC motor control consists of generating direct currents for motor phases. The current of the phase winding entering the segment in accordance with the commutation is forced to return to the direct current bus-bar by completing its path through the conjugate diode of the power switch, and thus it is extinguished.

During an electrical cycle of the system, that is, by obtaining six-step commutation and transmission equivalent circuit, state space differential equations modelling the motor are produced with the help of circuit analysis theory.

Figure 4 shows the drive system of BLDC motor. As it is seen from Figure 4, the motor and inverter block consist of three phase winding resistors, inductances and back EMFs. As it is seen in Table 2, the commutation ranges of the system were determined with six triggering pulses and the state-space equations of the operating states were developed as shown below [19-20].

As seen in Table 2, the equations for forming of the mathematical model in the transition from S5-S6 feeding step to S1-S6 step are as follows:

$$i_a + i_b + i_c = 0 \tag{1}$$

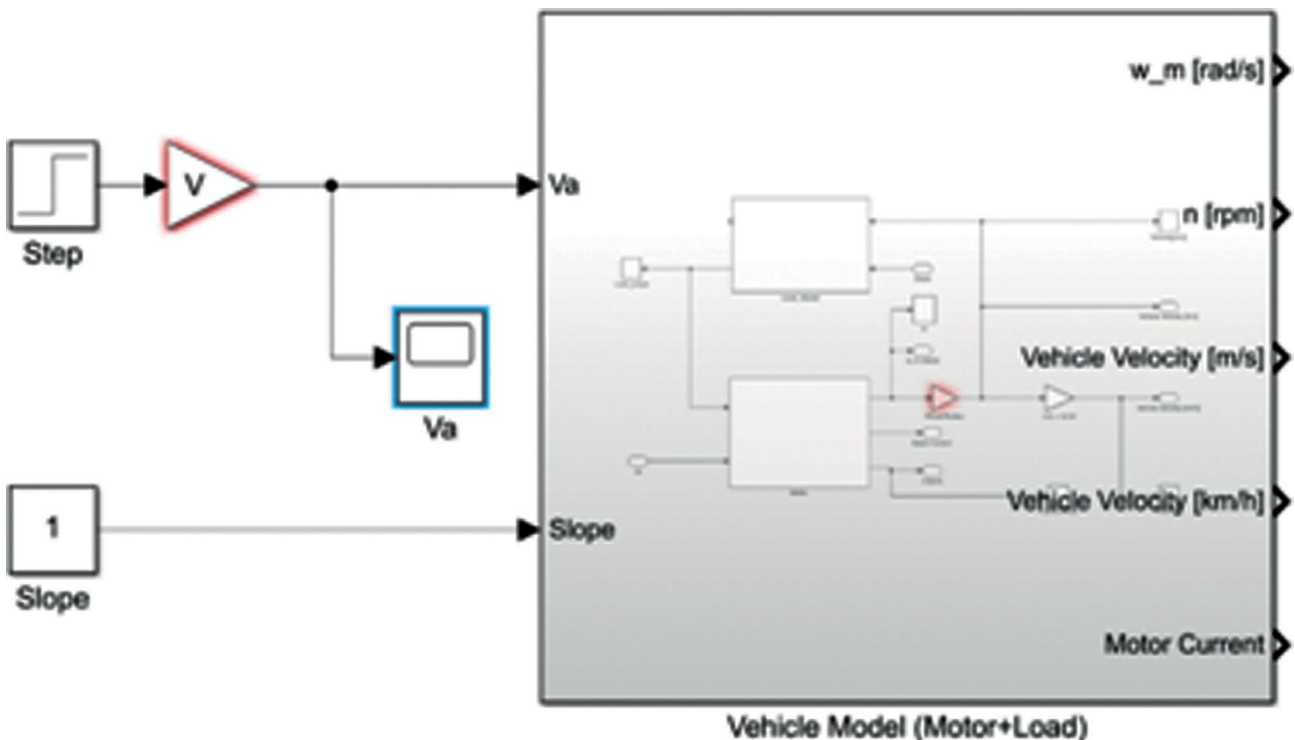$$0 = Ri_c + (L+M)\frac{di_c}{dt} + E_c - E_b - Ri_b - (L+M)\frac{di_b}{dt} \tag{2}$$
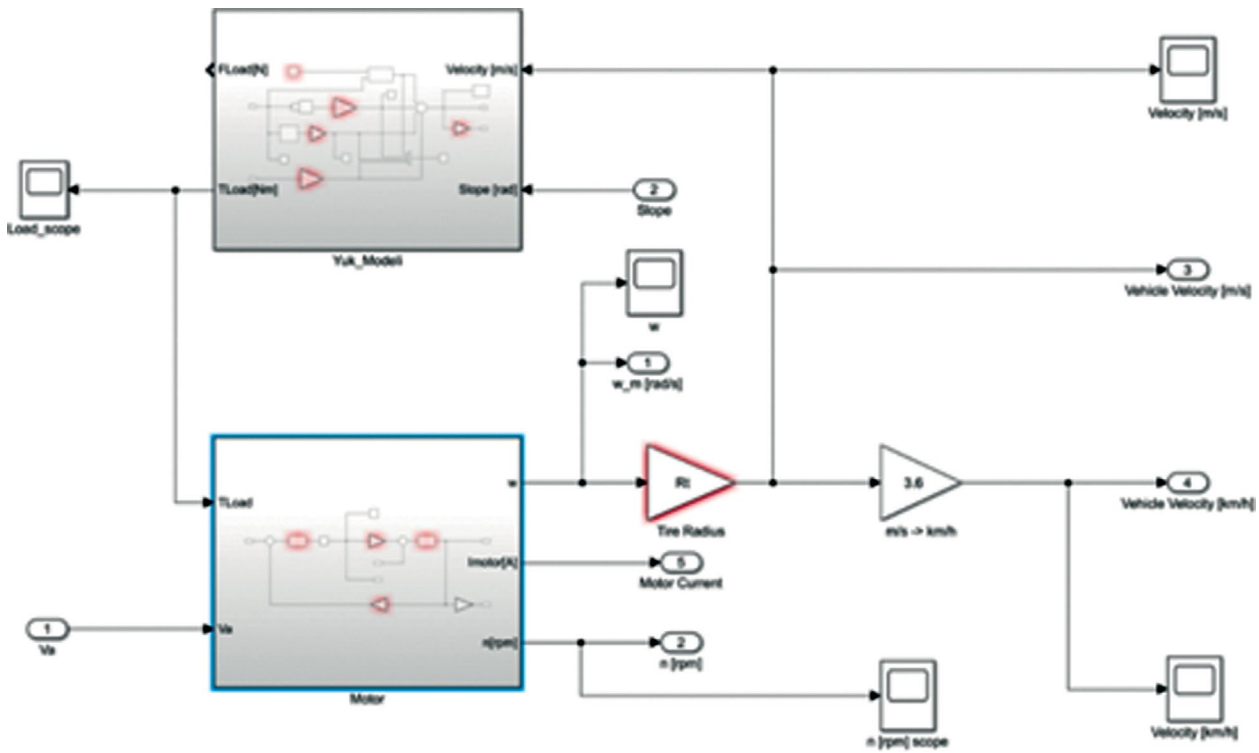

Figure 2. Vehicle general model.

Figure 3. Internal structure block of the general vehicle model.

Table 2. Conduction of switch pair with rotor position

Rotor Position	Conduction of Switch Pair
$\frac{\pi}{6} < \theta_r < \frac{\pi}{2}$	S1-S6
$\frac{\pi}{2} < \theta_r < \frac{5\pi}{6}$	S1-S2
$\frac{5\pi}{6} < \theta_r < \frac{7\pi}{6}$	S3-S2
$\frac{7\pi}{6} < \theta_r < \frac{3\pi}{2}$	S3-S4
$\frac{3\pi}{2} < \theta_r < \frac{11\pi}{6}$	S5-S4
$\frac{11\pi}{6} < \theta_r < \frac{\pi}{6}$	S5-S6

$$V_d = Ri_a + (L+M)\frac{di_a}{dt} + E_a - E_b - Ri_b - (L+M)\frac{di_b}{dt} \quad (3)$$

While S2-S6 semiconductor switches in Figure 4.b are in transmission, that is, equations numbered (1), (2), (3) are functional during the commutation period. When S1-S6 semiconductor switches are in transmission, current does not flow through the C phase and the following equation numbered (4) realizes. In this case, equation numbered (5) is obtained according to the new values of I_a and I_b. The following two equations are functional during the transmission period.

$$i_a + i_b = 0 \qquad (4)$$

$$V_d = Ri_a + (L+M)\frac{di_a}{dt} + E_a - E_b - Ri_b - (L+M)\frac{di_b}{dt} \quad (5)$$

In order to the mathematical model is completed at this step of the system, it is necessary to write the differential equations for motor mechanical model. The differential equation associated with the mechanical analysis side of electrical and mechanical analysis, expressed by equation (6)-(8), is valid for all feeding steps. The meanings of the symbols used in the equations in all mathematical expressions are shown in Table.3.
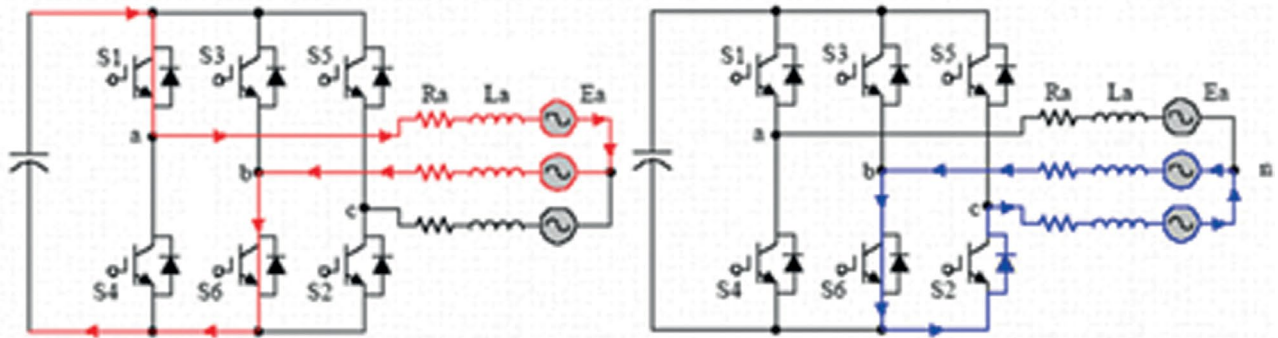
Figure 4. a) State space model circuit when S1-S6 in conduction, b) State space model circuit when S2-S6 in conduction (commutation).

Table 3. Motor Parameters

Nomenclature	
V_d	Applied Phase Voltage
E	Back EMF
i	Phase Current
R	Phase Resistance
L	Self-Inductance
ω	Angular Speed
B	Viscous friction constant
J	Moment of Inertia
T_y	Load Torque
M	Output Torque

$$M_m - M_y = j\frac{d\omega}{dt} + B\omega \qquad (6)$$

$$\frac{d\omega}{dt} = \frac{1}{(J_m + J_y)}\left[M_m - M_y - (B_m + B_Y)\omega \right] \qquad (7)$$

$$M_m(t) = k_a i_a + k_b i_b + k_c i_c \qquad (8)$$

The equivalent J and B values seen in the above expressions are $J = J_m + J_y$ and $B = B_m + B_y$

Analytical correlations of the voltages induced in each phase winding are defined for each feeding step in order the state space model of the whole system to be completed.
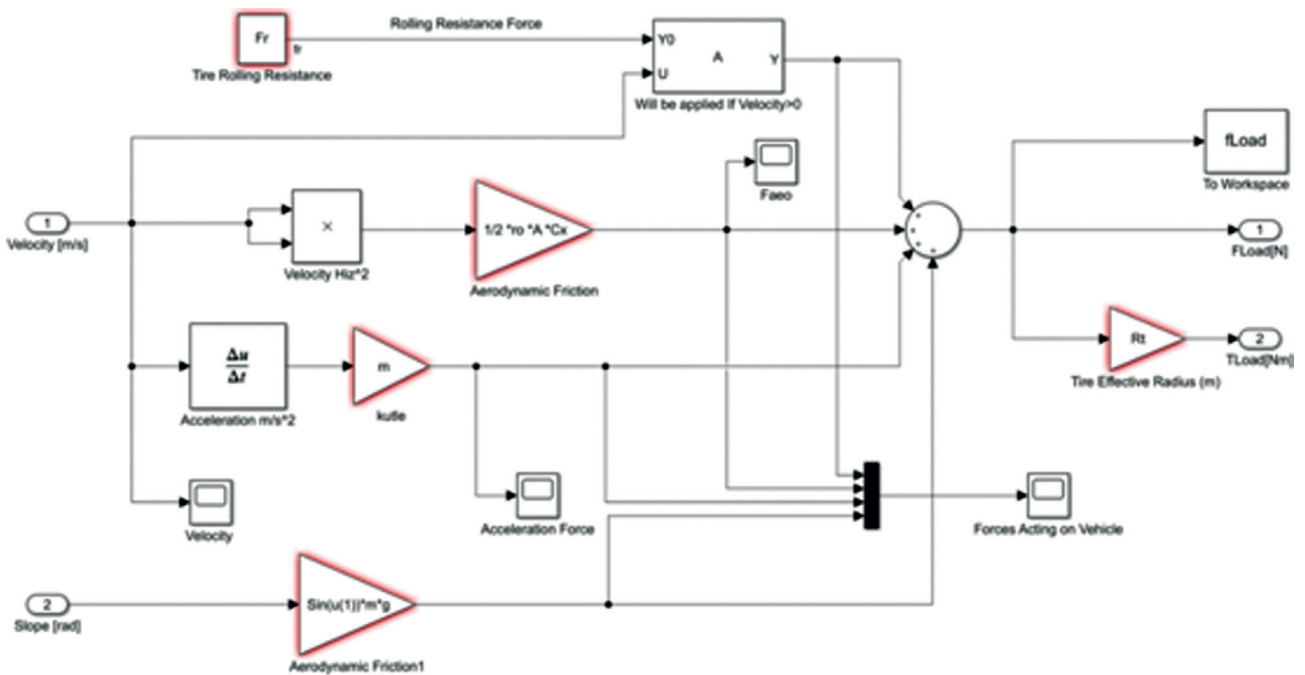

Figure 5. BLDC Motor Model.

Figure 6. Load model.

The current equation is given for a brushless dc motor as Equation (9).

$$\frac{d}{dt}\begin{bmatrix} i_1(t) \\ i_2(t) \\ i_3(t) \end{bmatrix} = \begin{bmatrix} -\dfrac{R}{L} & 0 & 0 \\ 0 & -\dfrac{R}{L} & 0 \\ 0 & 0 & -\dfrac{R}{L} \end{bmatrix}\begin{bmatrix} i_1(t) \\ i_2(t) \\ i_3(t) \end{bmatrix} + $$
$$\begin{bmatrix} -\dfrac{1}{L} & 0 & 0 \\ 0 & -\dfrac{1}{L} & 0 \\ 0 & 0 & -\dfrac{1}{L} \end{bmatrix} \cdot \left(\begin{bmatrix} V_1 \\ V_2 \\ V_3 \end{bmatrix} - \begin{bmatrix} e_1(t) \\ e_2(t) \\ e_3(t) \end{bmatrix} \right) \quad (9)$$

Detailed block diagram of the BLDC motor is shown in Figure 5. Here, a current limiting block with a value 1.5 times the nominal motor current was placed at the output of the motor impedance block. The maximum current that the direct current source can give or the current limit of the driver circuit can be modeled with this limiting block.

When the gearing ratio is 1, all forces acting the vehicle and the load moment affecting the motor shaft can be modeled as in Figure 6. Here, the tire rolling resistance is indicated by a constant block as it is a constant force. The *fcn* function block, which is connected to the tire rolling

Table 4. Parameters of the BLDC motor and power system

Parameter	Value	Unit	Definition
V_Buss	375,0	Volt	Busbar Voltage
Lq	0,6	mH	2 phase inductances
Rq	0.1634	Ohm	2 phase resistance
Kp	1,55	Nm/A	Moment Constant
Ki	1,55	Volt.s/rad	Back EMF Constant
Jm	0,341	kg.m^2	Motor Moment of Inertia
In	200	A	Nominal Current
Pn	75	kW	Motor Power

resistance force output, is a function block that will activate the function when the vehicle speed is higher than zero. All parameters such as aerodynamic friction, the vehicle mass, the slope of the road on which the vehicle is driven, tire rolling resistance, wheel diameter and the desired reference speed information were included in the calculations in the load model.

ELECTRIC VEHICLE CONTROL SYSTEM

In consideration of the requirements for the vehicle, the necessity of a 75kW drive power has emerged and the BLDC motor required for this has been determined and
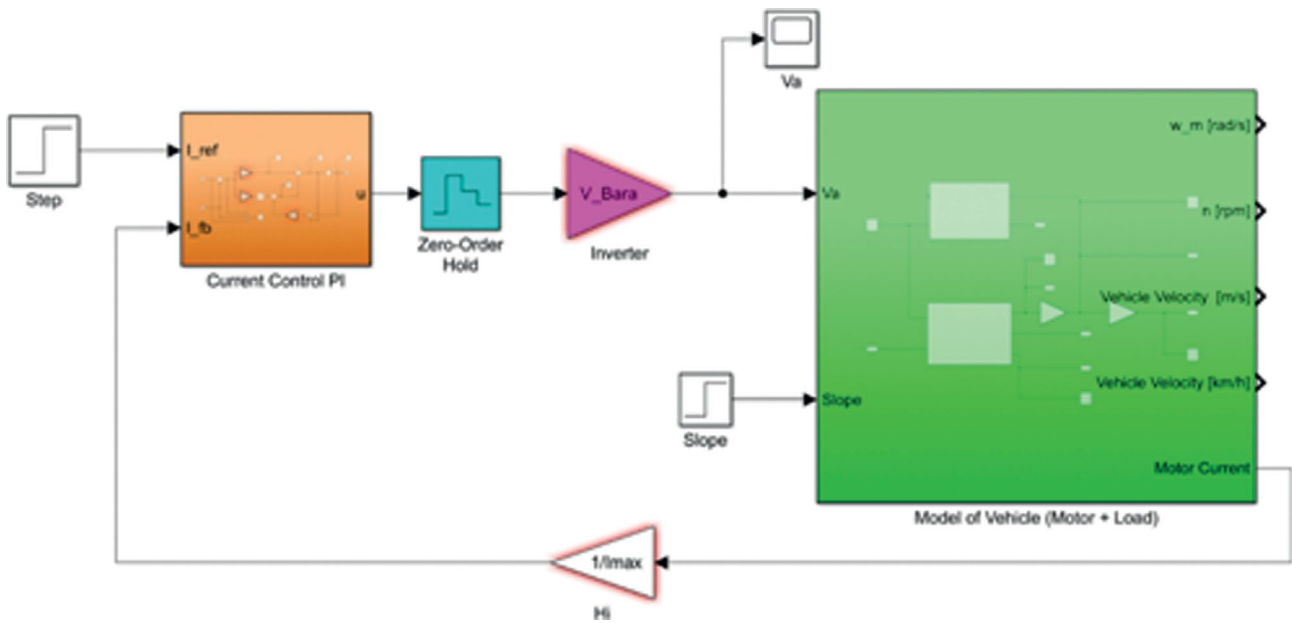
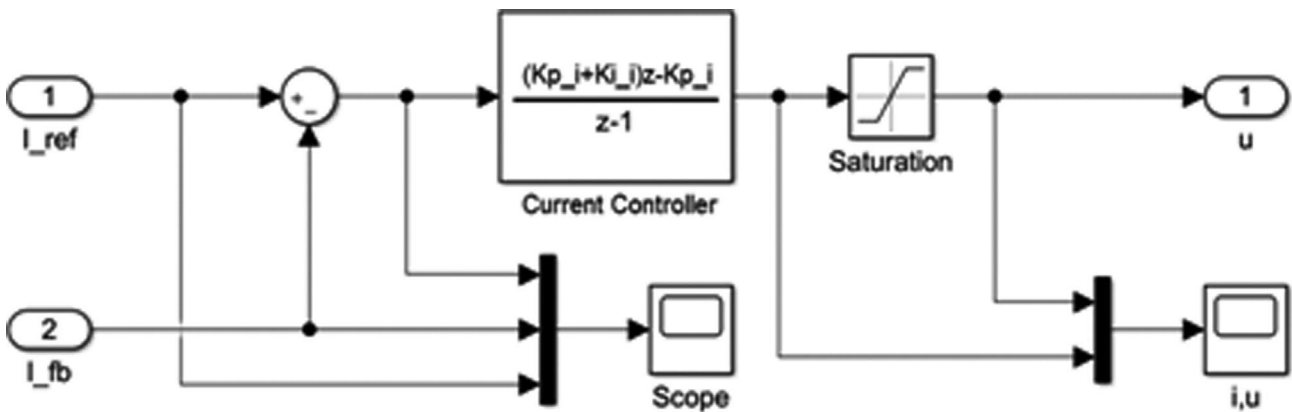**Figure 7.** Electric Vehicle Model with the Current Controller.

Figure 8. Internal structure of discrete current controller block.

its parameters have been obtained. Current voltage values of suitable switching components that can be used in the power stage that will drive this electric motor have been determined. For this purpose, 375V has been preferred for the feeding voltage of the 200A switching element. The parameters of the motor and power system are given in Table 4.

Current Control with PI Controller of BLDC Motor

The vehicle model is arranged according to the current controller as seen in Figure 7. The error signal was calculated with the current feedback signal from the electric motor and the reference signal. These formed the inputs of the discrete controller. The zero-order hold and the discrete

signal at the controller output have been continuously applied to the system. The sampling time of the block was adjusted from the "summing" block parameters, which take the difference of the feedback signal coming from the continuous system and the continuous reference signal, and a discrete error signal was created.

The feedback signal coming from the current controller block should be scaled and given to the controller input. Figure 8 shows the internal structure of the current control block. The current error value is obtained by subtracting the feedback current (I_{fd}) value from the reference current (I_{ref}) value.

The step response of the current control system is given in Figure 9. In the figure, it is showing the blue-colored

curve as the reference current, the green-colored curve as the output current and the red-colored curve as the discrete error signal. Steady-state error may occur if momentum is not applied to the motor in the current control system,
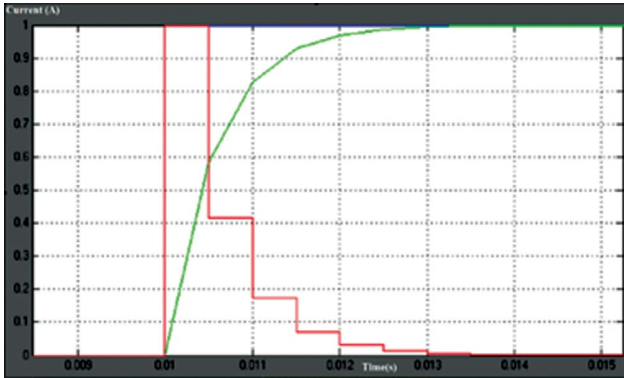

Figure 9. The step response of vehicle model.

especially at high current references. This can be seen when the acceleration is very close to zero after the vehicle speed reaches its maximum value. Since the vehicle does not accelerate, the momentum applied to the motor shaft will decrease, so the motor will draw less current. The controller will need to increase the motor's control signal in order to reach the requested reference value (the accelerator pedal of the vehicle). First of all, PI controller was used in the current control block and the controller will take the continuous integral of the increasing error due to its structure and the control signal will gradually increase. But since the control signal will be saturated after a certain value, wrapping will occur after a while. To prevent this situation, an unwrapped controller should be created.

In the PI controller, the constrained control signal is subtracted from the unconstrained control signal and multiplied by an appropriate coefficient and added to the control signal coming from the integral term. Thus, when the winding is formed, the control signal created by
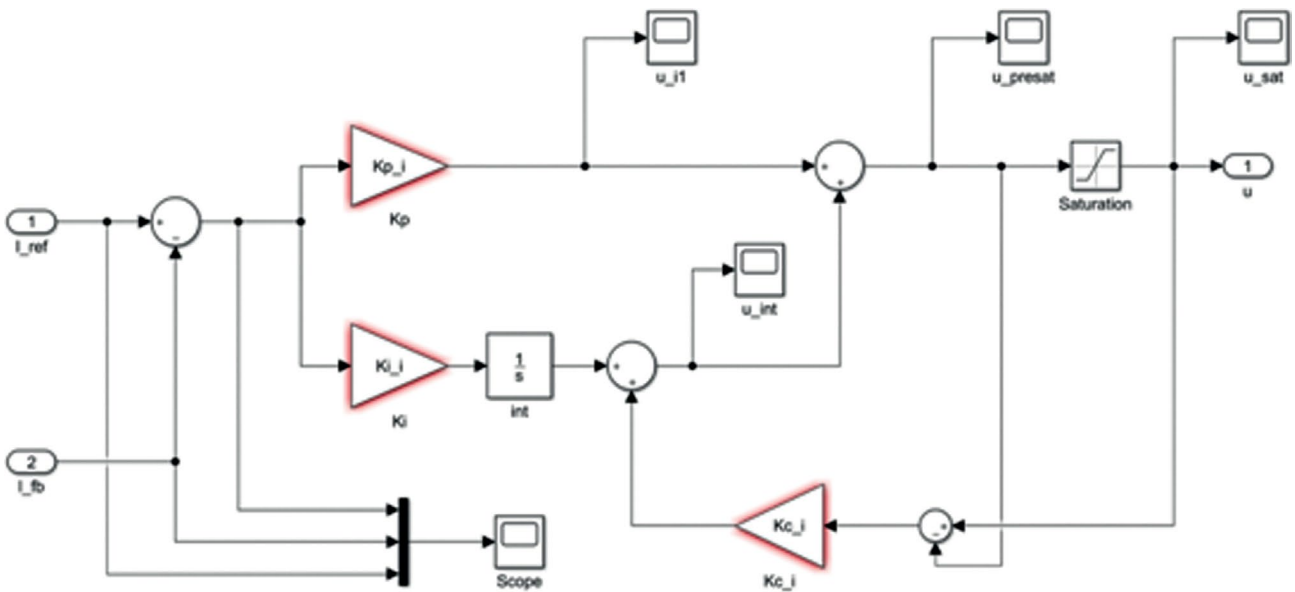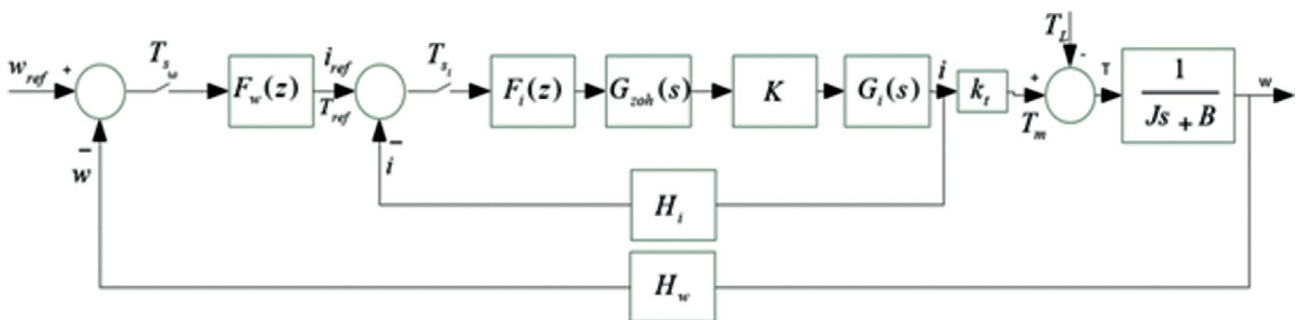

Figure 10. PI controller structure.

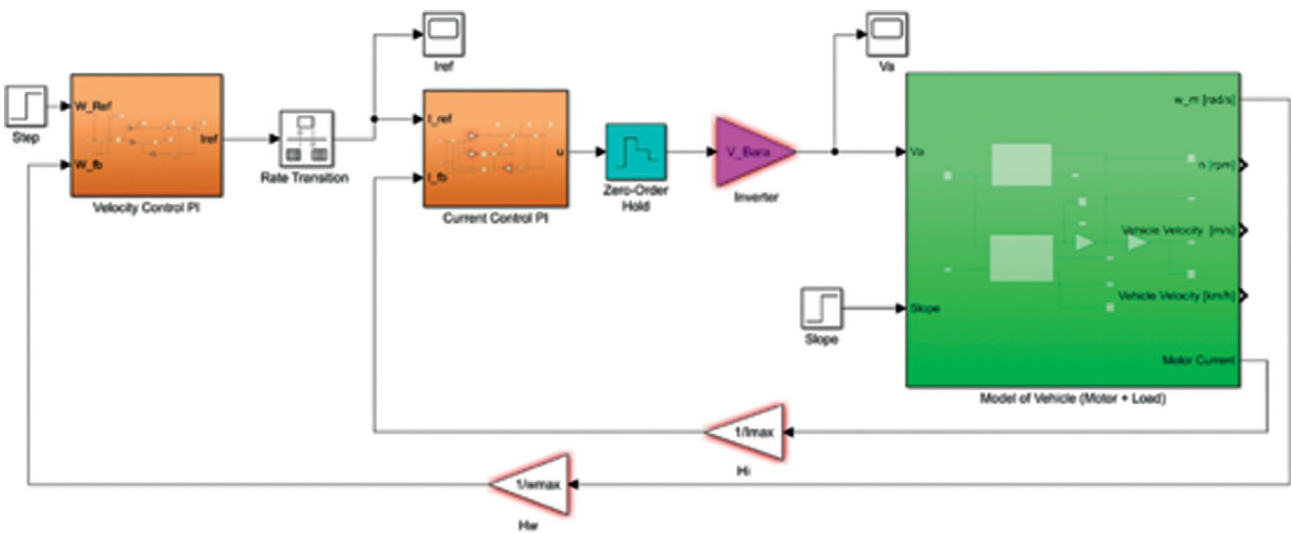**Figure 11.** Speed controller block diagram in cascade structure.

Figure 12. Vehicle model with cascade velocity and current controller.
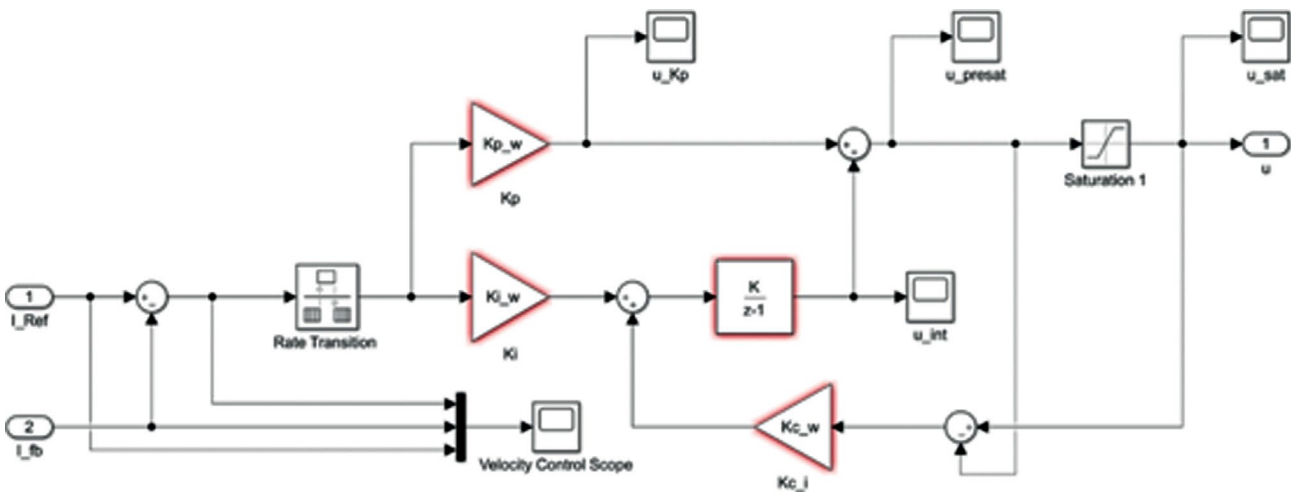

Figure 13. PI speed controller.

the integrator will decrease and the effect of the winding will disappear. Controller structure can be created as in Figure 10.

In this structure, if the signal between the input and output of the restriction element is the same, in other words, if the control signal is not saturated, the difference between these two signals will be zero and there will be no change in the controller's act.

PID based BLDC Motor Speed Control

Driving at a constant speed is important for energy efficiency in electrical vehicle. The energy consumed by a vehicle while accelerating is much more than a vehicle traveling at a constant speed. Various cruise control systems, which provide constant speed in vehicles, save energy by trying to drive the vehicle at the demanded reference speed. This

structure gives a torque reference to the system in electric vehicles as well as in internal combustion engine vehicles. The cascade speed controller sends the torque reference it creates to the current controller to keep the vehicle at the desired reference speed. The cascade control structure created in this study is shown in Figure 11.

Parameters proportional (P), integral (I), derivative (D) [21] connected in parallel will produce PID control. The transfer functions of the PID control are as equation 10. In industrial and automotive applications, PID controllers expressed as equation (10) are effective controllers that are widely used in the time unvarying linear system [22-25].

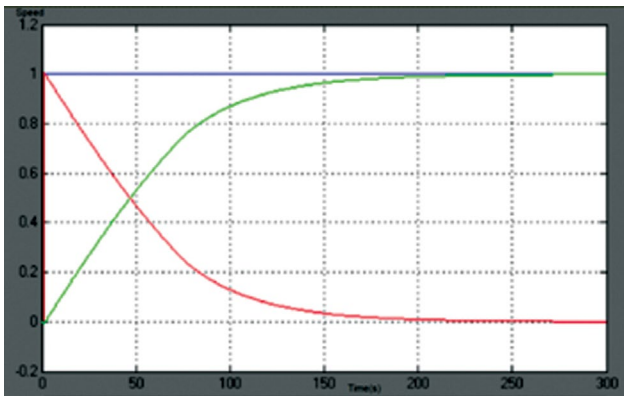$$u(s) = [K_p + \frac{k_i}{s} + s \ K_D]E(s) \qquad (10)$$

Figure 14. The vehicle's response to step input.

Here is defined as T is the sampling period. Also, as can be seen from equation (10), the design parameters of the PID controller are specified with the expressions of proportional gain (Kp), integral gain (Ki) and derivative gain (Kd). PID control has the characteristics of increasing the rise time, reducing the steady-state error, and reducing oscillations [26]. PID control structure was designed by assuming the derivative term gain as zero in the above equation. The controller must contain an integral term so that the system does not generate a steady-state error due to the distortionary load effects that cannot be added to the forward path model. It will be enough to design a PI controller according to the 1st degree transfer function obtained.
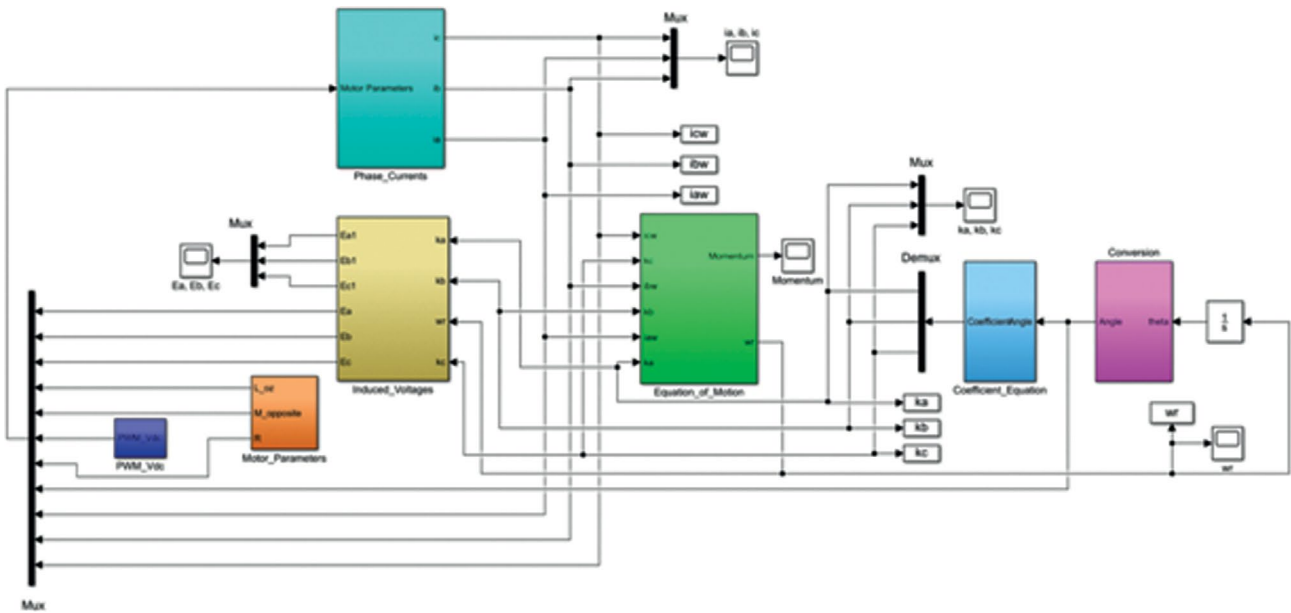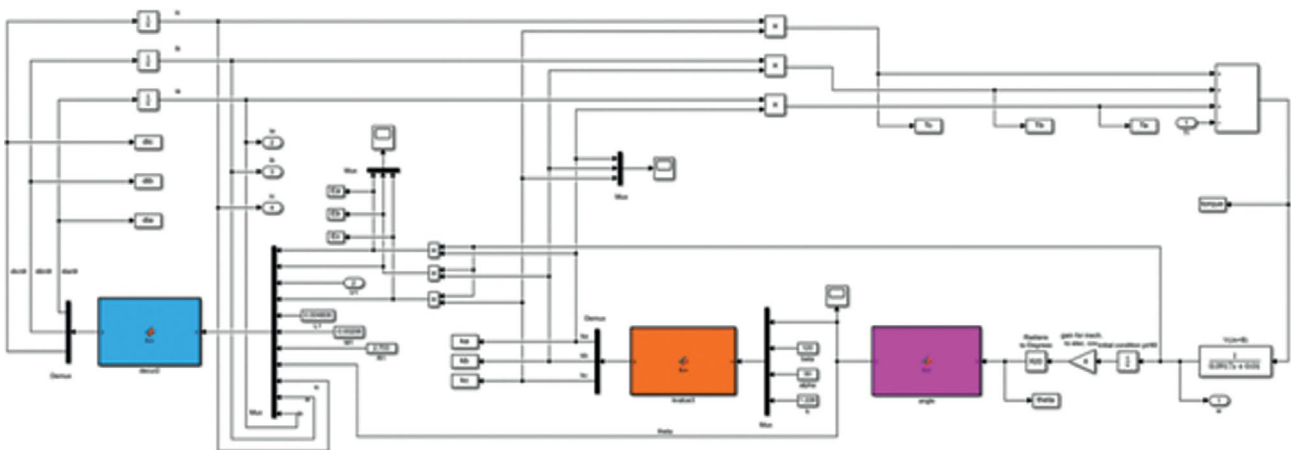

Figure 15. Simulink model of BLDC motor.

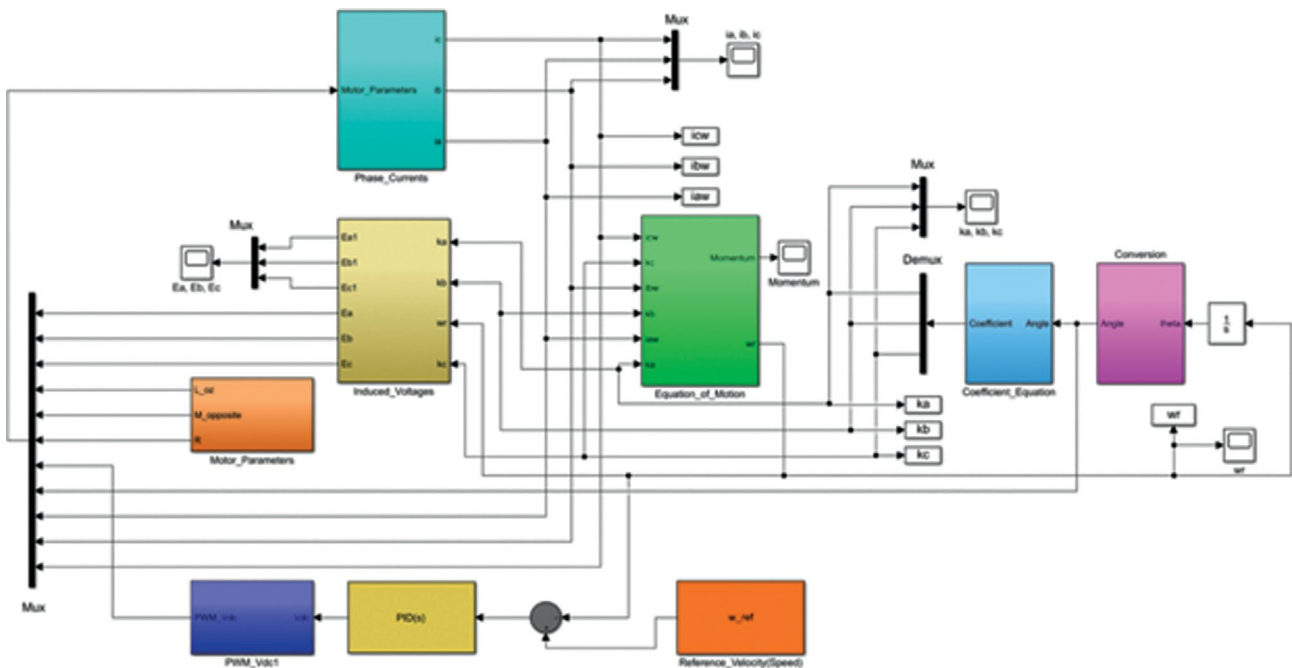**Figure 16.** Simulink model of the BLDC motor controller.

Figure 17. PID control of the BLDC motor.

The system pole may be displaced due to changing inertia and viscosities. The controller to be designed must be resistant to variations in the model. In discrete time controller design, a zero is assigned to the left side of this pole in order to eliminate the effect of the pole that is very close to z=1 of the system. In the design made with pole and zero assignment with the help of MATLAB SISO tool, the discrete time controller was selected with this way below;

$$F_\omega(z) = 100 \frac{z - 0.987}{z - 1} \qquad (11)$$

If this function in the equation (11) is rewritten according to Kp and Ki values, the equation (12) is obtained.

$$F_{P1}(z) = \frac{z(K_p + K_i) - K_p}{z - 1} \qquad (12)$$

In this study, the best value selected as optimized was found through experimentation in the simulation. Kp and Ki coefficients were found as K_p=98.69 K_i=1.3,

In the system model created in MATLAB/Simulink environment, the cascade structure can be completed by bringing a speed controller in a way to give to reference the current control block. For the speed controller, the feedback received from the motor speed must be scaled and sent to the speed controller. Due to the sampling frequency of the speed control system is different from that of the Current control, "Rate Transition" blocks in MATLAB Simulink are used. The ratio between two sampling frequencies is 1000.
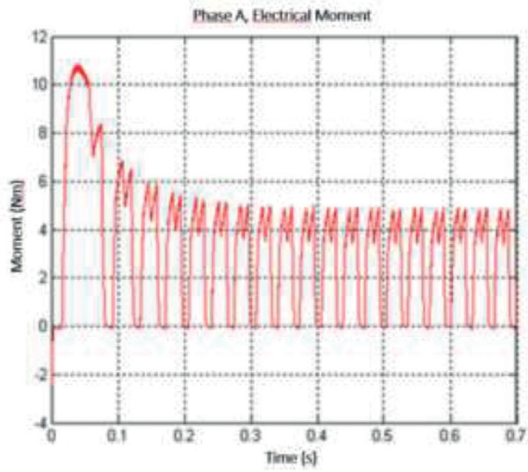
The controller block is completed by arranging the unwrapped controller structure as shown in Figure 12 and its internal structure as shown in Figure13. The step response of the system with the obtained control parameters was as shown in Figure 14. The reference input is represented by the blue curve and the response output of the system by the green curve. The error between the reference value and the output of the system is represented by the red colored curve. The error is determined by the difference of the actual velocity and the reference.

Simulink model of BLDC motor was realized as seen in Figure 15. Simulink model of the BLDC motor controller is designed as shown in Figure 16.
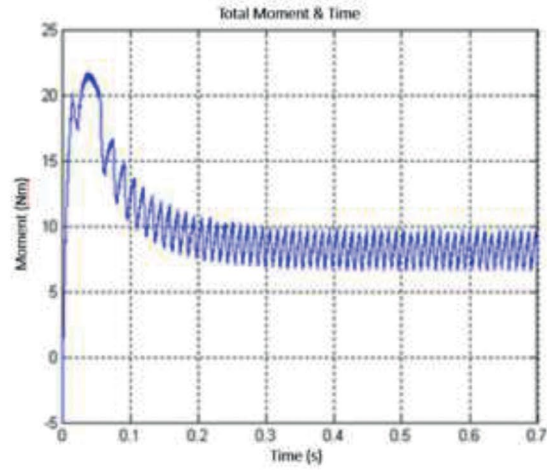
Then as second controller, PID control of the BLDC motor is designed as in Figure 17. Kp, Ki, Kd values, which give the best results in BLDC motor PID controller design, were determined as Kp = 98.69, Ki = 1.3, Kd = 1 by experiments.

By creating transform blocks in MATLAB/Simulink environment, position and velocity data are obtained by using motion, velocity equations. The torque data of the motor is obtained by phase currents. Sub-blocks are used to create the simulation model such as equations of motion, motor coefficient equations, phase currents, phase voltages, motor parameters.
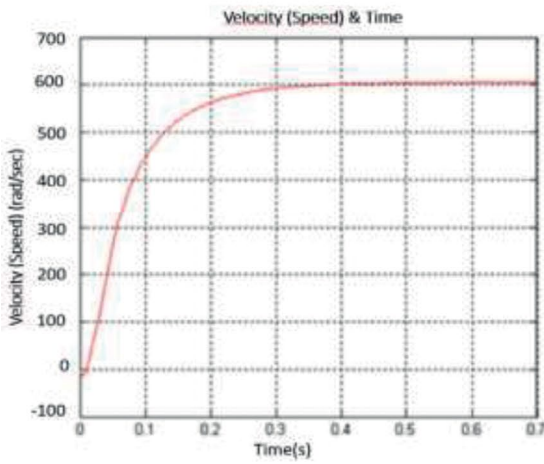
The performance results of the BLDC motor obtained by simulation are shown in Figure 18. Figure 18(a) shows
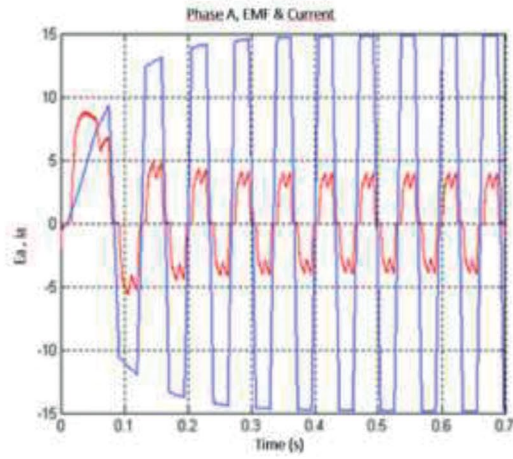
a) Moment time graph of phase A
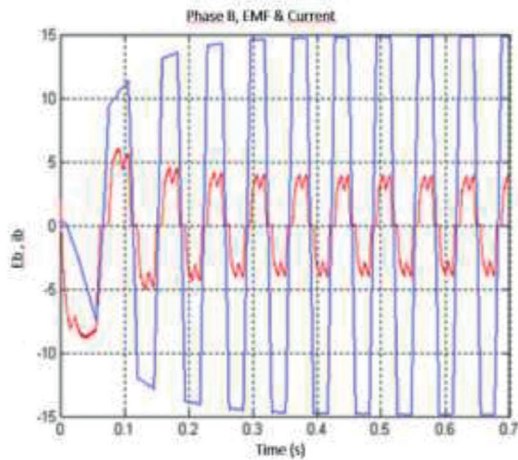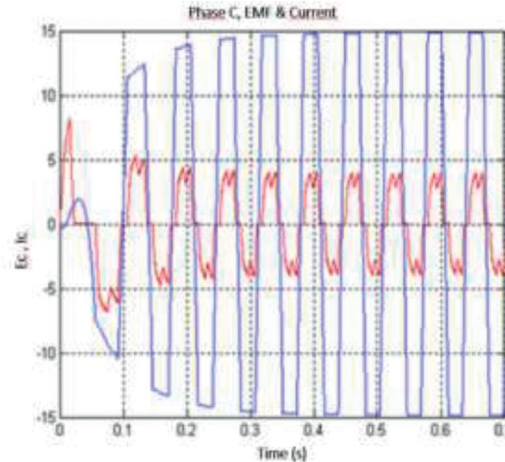

b) Total moment time graph of BLDC motor

c) Velocity (Speed) versus time graph of BLDC motor

(d) Back EMF Ea (V) and current Ia (A) versus time graph of phase A

(e) Back EMF Eb (V) and current Ib (A) versus time graph of phase B

(f) Back EMF Ec (V) and current Ic (A) versus time graph of phase C

Figure 18. Performance results of the BLDC motor by simulation.

the change electrical moment versus time on Phase A. Figure 18(b) shows the change total moment versus time. Figure 18(c) shows the change velocity (speed) versus time for a reference speed of 600 rpm of BLDC motor. Figure 18 (d) shows the simulated motor current and back EMF in phase A for a starting transient under PID control, based on Equation (1)–(9) with non-zero rotor flux for a constant load. Likewise, back-EMF and current graphs of phase B in figure 18(e) and phase C in figure 18(f) are shown.

Speed Control with Fuzzy Logic Controller of BLDC Motor

The desired reference speed is applied to the system with the accelerator pedal of the vehicle. The voltage applied to reach this reference value is adjusted to control the speed of the BLDC motor. The difference between the actual speed and the reference speed is called the error. The applied voltage is changed by increasing or decreasing the duty cycle in order to minimize the error of power semiconductors.

In this study, fuzzy logic controller has been applied to the general model of BLDC motor in the MATLAB/

Simulink Fuzzy Logic Toolbox. The proposed fuzzy logic control circuit is shown in Figure 19. The fuzzy logic process takes place in three steps, which are fuzzification, inference and defuzzification are performed using the MATLAB Fuzzy Logic Toolbox. In the study, the five labels in Table 5 for each input value in the fuzzification process are defined as membership functions. The fuzzy speed controller of the BLDC motor contains two separate blocks of rules. The inputs of the first block are the speed error (e) is shown in Figure 20 and the change in the speed error (ce) is shown in Figure 21. The output of the first block is the calculated voltage change (cvi) is shown in Figure 22 which is also the input of the second block. Another input to the second block is the highest line current (i) is shown in Figure 23 of the motor at that moment. The output of the second block is the applied voltage change (kcv) [27].

The determined speed rule bases of Fuzzy logic control structure are shown in Table 6, and the current rule bases are shown in Table.7. The rule base of the fuzzy logic system is realized by creating IF-THEN rules [28]. The fuzzy speed controller of BLDC motor includes two separate rule blocks [29].

In the fuzzy logic speed control system, even if the load variances, the BLDC motor's speed will operate in the steady state at 500 rpm (reference speed). This restriction is provided through the fuzzy logic controller. The error is calculated by subtracting the reference speed and the current speed. The error variance is calculated by considering the difference between the current error and the error of the previous sampling period. Based on the error and the error variance, the first block of the fuzzy logic controller calculates a voltage variation (cvi). The second block of Fuzzy

Table 5. Membership function label.

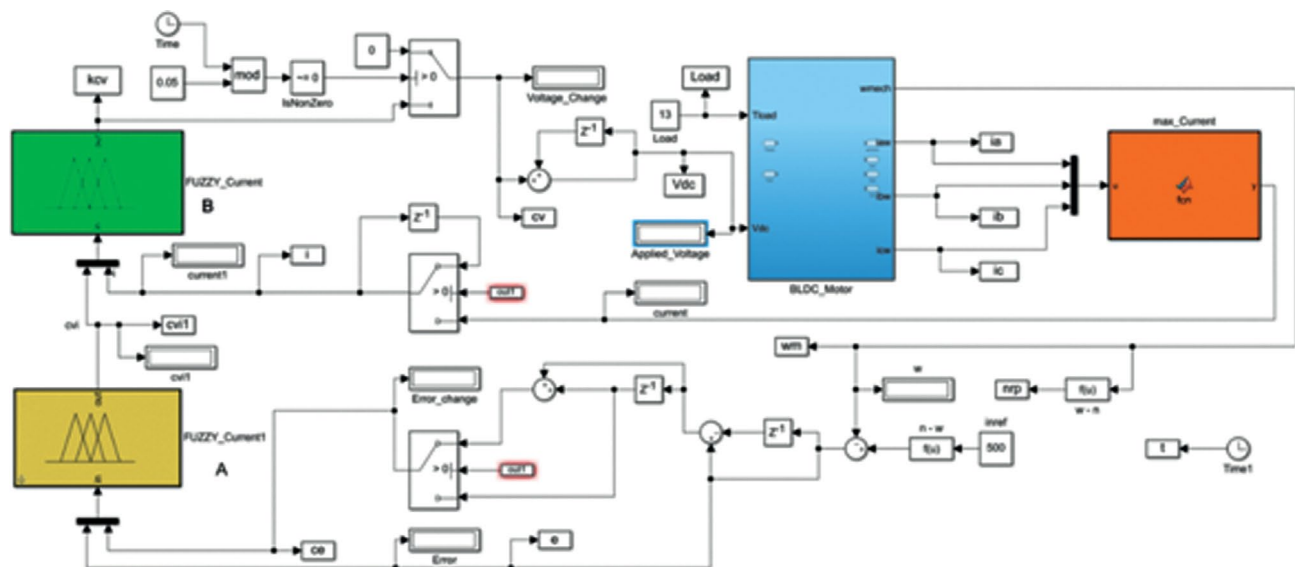| Membership Function	Notation
Positive Big	PB
Positive Small	PS
Zero Environ	ZE
Negative Small	NS
Negative Big	NB

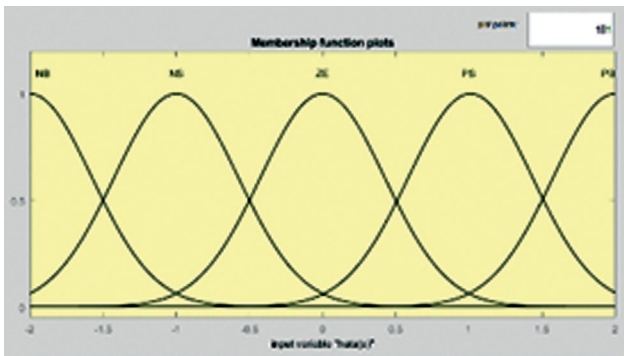**Figure 19.** The proposed fuzzy logic control circuit.

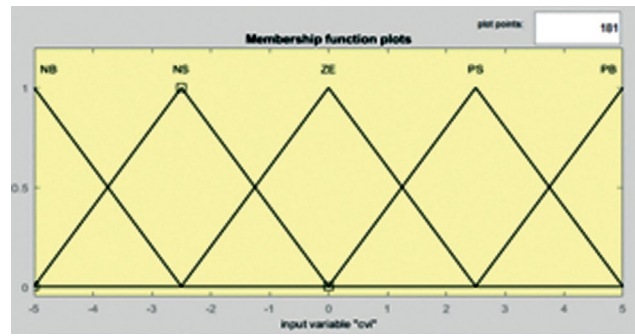**Figure 20.** Membership functions in regards to the speed error (e).

Figure 22. Membership functions in regards to the variation of calculated and applied voltages (cvi).
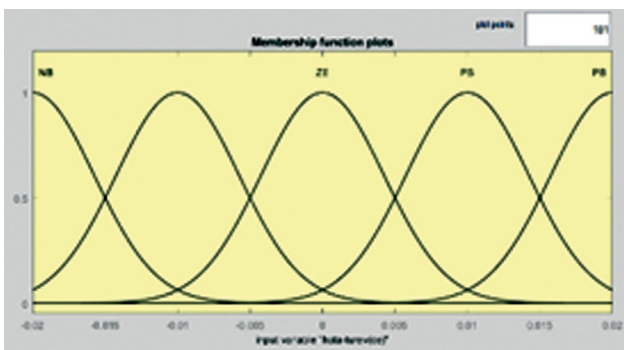

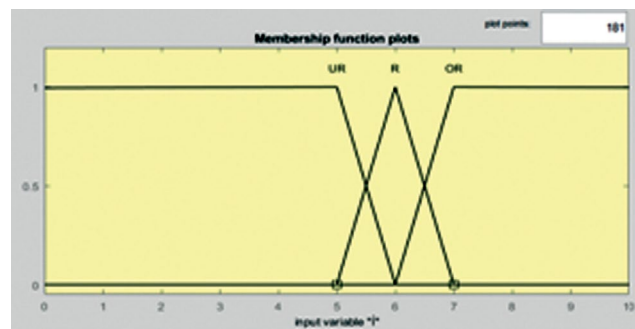**Figure 21.** Membership functions in regards to the speed error variance (ce).

Figure 23. Membership functions in regards to the current (i).

Table 6. Fuzzy Logic Controller speed rule

e \ ce	NB	NS	ZE	PS	PB
NB	NB	NB	NB	NS	NS
NS	NB	NB	NS	NS	NS
ZE	NB	NS	ZE	PS	PB
PS	PS	PS	PS	PB	PB
PB	PS	PS	PB	PB	PB

Table 7. Fuzzy Logic Controller current rules

i \ cvi	NB	NS	ZE	PS	PB
UR	NB	NB	NB	NS	NS
R	NB	NB	NS	NS	NS
OR	NB	NS	ZE	PS	PB

Control calculates the voltage variation that should be applied to the BLDC motor by considering the calculated voltage variation and the current of the BLDC motor. This procedure is very important to protect the BLDC motor and prevent the motor overcurrent draw. The center-of gravity method has been used in the defuzzificiation process.

SIMULATION AND EXPERIMENTAL RESULTS

For practical application, the dSPACE DS1401 Digital Signal Processing unit was used for BLDC motor Rapid Control Prototyping. DS1401 DSP working rhythmically with MATLAB/Simulink blocks is transmitted to the processor as hex code by converting Simulink blocks directly to C code.

Additionally, the system has been producing the control signals required by the signal processing procedure, as well. DS1401 system can be directly connected to our computers via Ethernet connection and can operate the MATLAB/Simulink blocks we developed by recognizing the hardware. In the MATLAB/Simulink structure, these system drivers are available and directly seen in the system.
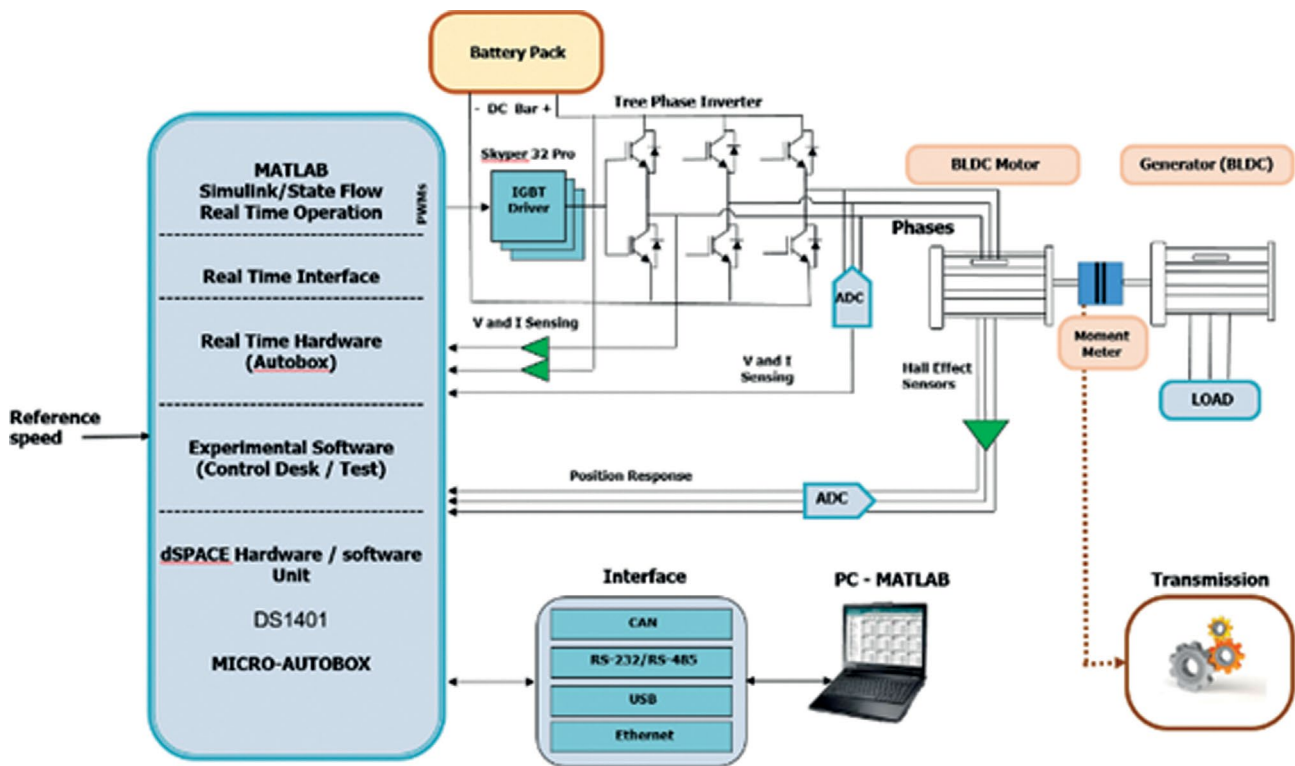
Figure 24. BLDC motor's rapid control prototyping block diagram with dSPACE MicroAuto-Box.

Figure 25. 75 kW liquid-cooled, fully-controlled three-phase DC-AC converter and control system experimental setup.

The I/O definition is made very easily in the section called Real-Time Interface (RTI). These software blocks can control the motor driver through DS1401 system CAN-BUS, RS485 ports.

MATLAB/Simulink blocks are seen in the PID control system in Figure 15 and Figure 17 and the fuzzy logic control system in Figure 19. These control blocks have been loaded into the dSPACE control structure. A real-time control setup has been created between the prepared HIL (Hardware in the Loop) system with the power stage and the PC via dSPACE. Here, HMI (Human-Machine Interface) interface has been prepared to provide real-time

Figure 26. PID and Fuzzy Controller Speed-Time Curve.

Figure 27. PID and Fuzzy Controller response at resistance change and sudden load.

intervention to the whole system via PC. A GUI has been designed on the PC to optimize and monitor the controller parameters real-time.

A very good solution has been created for rapid prototyping with this HIL system. The block diagram of this system is shown in Figure.24. Developed control algorithms have been tested with this rapid prototyping. This testing platform is shown in Figure.28.

Motor modelling was designed using simulation programs according to the basic parameters of the vehicle, and the electric motor was selected as a result of the power calculation. The PI, PID and fuzzy logic controller of this selected motor (BLDC) was designed with the rapid control prototyping method. By loading the Simulink model of the BLDC motor, the fuzzy logic controller was designed and loaded into this model which was transmitted directly with a DSP via the DS1401 dSPACE digital signal kit after the PI and PID controller in a structure that controls the voltage and current. Factors such as speed error used in fuzzy logic control structure, determination of variation in speed error, calculation of voltage error according to the variation in speed and speed errors enable to cope with parameter variations and load disturbances. This type of controller is more durable and faster than other traditional control techniques.

PID and fuzzy controller speed-time curve simulation result of BLDC motor is shown in Figure 26. The simulation result of PID fuzzy controller response in resistance change and inrush load curve is shown in Figure 27. In Figure 26 simulation results were taken at 500 rpm motor speed value, Kp = 98.69, Ki = 1.3, Kd = 1 as a reference. At these values, the PID controller reached the reference value (500 rpm) in 0.24 seconds and the fuzzy controller reached controller output value in 0.044 seconds. The criterion values are given in Table.8 by comparing PID, fuzzy controllers.

Table 8. PID, Fuzzy Controller comparison

Criterion Values	PID	Fuzzy
Settling Time Ts (sn)	0.24	0.044
Rise Time T_r (sn)	0.075	0.015
Time difference for Loading Δt	0.44	0.04
Overshoot (%)	3.7	0
Steady-State Error e_{ss}	0	0
Steady-State Error While Loading e_{ss}	0	0.001
İntegral Square Error (ISE)	0.0372	0.00732
İntegral Absolute Error (IAE)	0.0584	0.0103212

As it is shown in Table 8, it can be seen that a fuzzy controller successfully controls the BLDC motor and the model-based programming of DSPs is very simple and versatile when compared to traditional methods, and the proposed fuzzy logic controller performs better than the PI technique. Experimental results show that the proposed fuzzy logic control method better compensates for the effects of time-varying load, while reducing steady-state error more than other methods as time progresses. The tests of BLDC motor's PID and fuzzy logic controller algorithms were applied as a practical application in the electric vehicle HIL system, as well. As it is seen in Figure 25, "originally designed 75 kW liquid-cooled, fully controlled, three-phase DC-AC converter", oscilloscope, power sources and computer were used as other parts of this HIL system.

The fuzzy logic control method has been observed to provide better control by updating the control parameters constantly and repeatedly.

Hence, DC motor in HIL structure in Figure 28, DC generator, DS1401 dSpace MicroAuto-Box, CAN-BUS

Figure 28. System motor-generator test platform with DS1401 dSpace MicroAuto-Box.

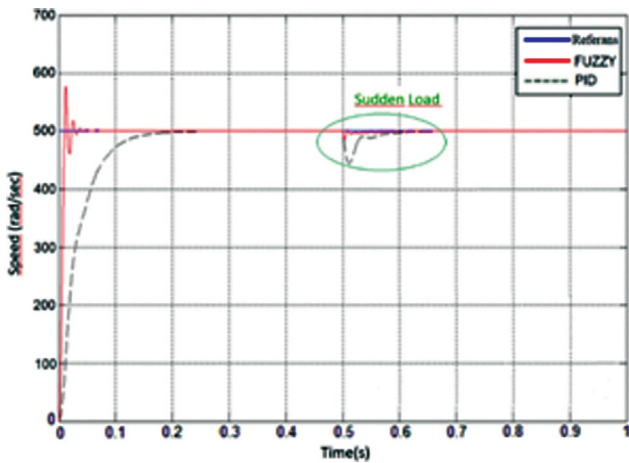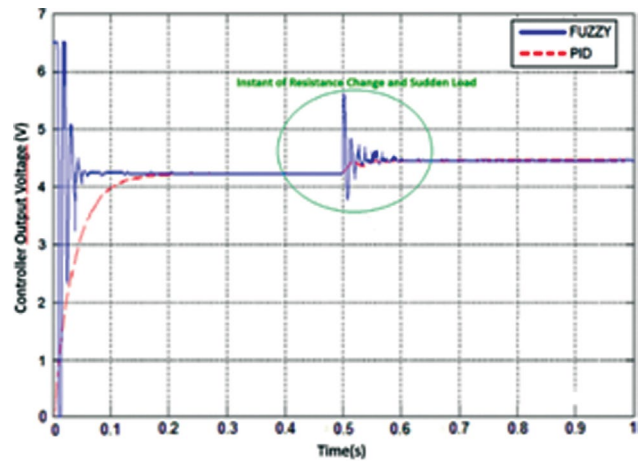**Figure 29.** 75 kW liquid-cooled, fully-controlled three-phase DC-AC converter and control system on platform (car).
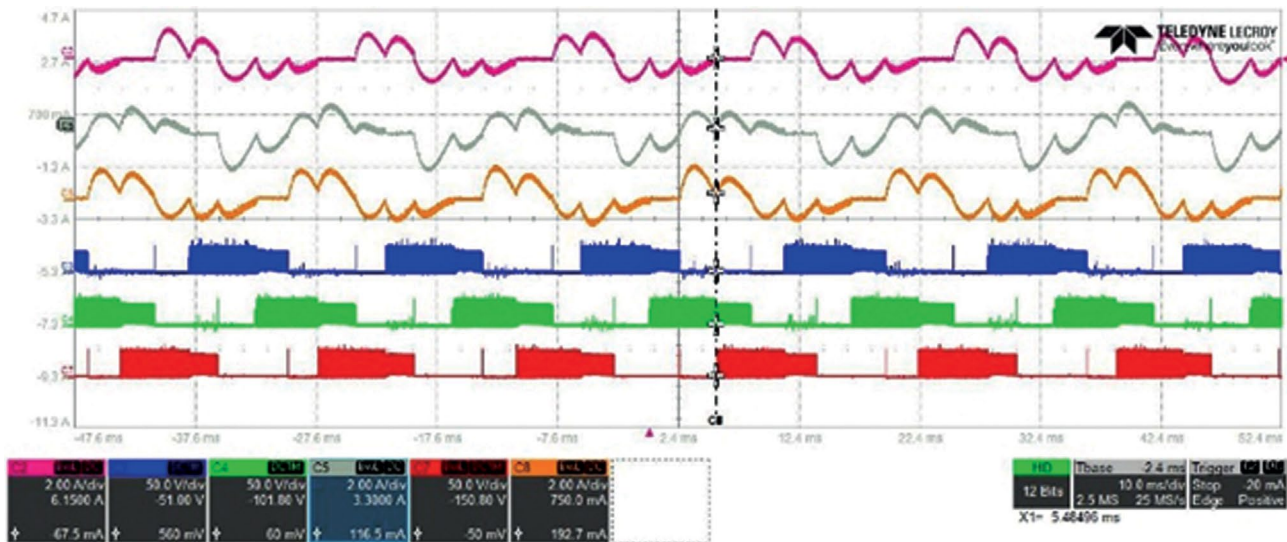

Figure 30. BLDC motor phase currents (I_{f1} Burgundy, I_{f2} Gray, I_{f3} Orange), BLDC motor interphase voltages (V_{23} Blue, V_{12} Green, V_{13} Red).

Communication, PC connections, DC power source, DC motor driver, liquid cooling system were used.

Figure 29 shows the 75 kW liquid-cooled, fully-controlled three-phase DC-AC converter and control system, with BLDC motors and gearbox (transmission system) mounted on the vehicle.

The performance and accuracy of the algorithms have been tested in practice and BLDC motor phase currents (If1 Burgundy, If2 Gray, If3 Orange), BLDC motor interphase voltages (V23 Blue, V12 Green, V13 Red) were monitored with oscilloscope as in Figure 30.

When the BLDC motor slows down, stops and the vehicle goes down the ramp, it damages the back-EMF power

modules. The following measures should be taken for the safe and stable operation of the developed control algorithms. Firstly, protection diodes should be connected to the terminals of the power semiconductor as in figure 31. Also, when back-EMF occurs; The power semiconductor T_1 must be turned on and this energy must be converted into heat on the load resistor R_L shown in figure 32. Addition to this control software can be achieved with an algorithm. For this, software development was carried out in the study.

Snubber capacitances ($C_{snubber}$) should be connected to the inputs of the power semiconductor modules as seen in figure 31. Snubber capacitances are used to prevent overvoltage surges that occur on power switching modules
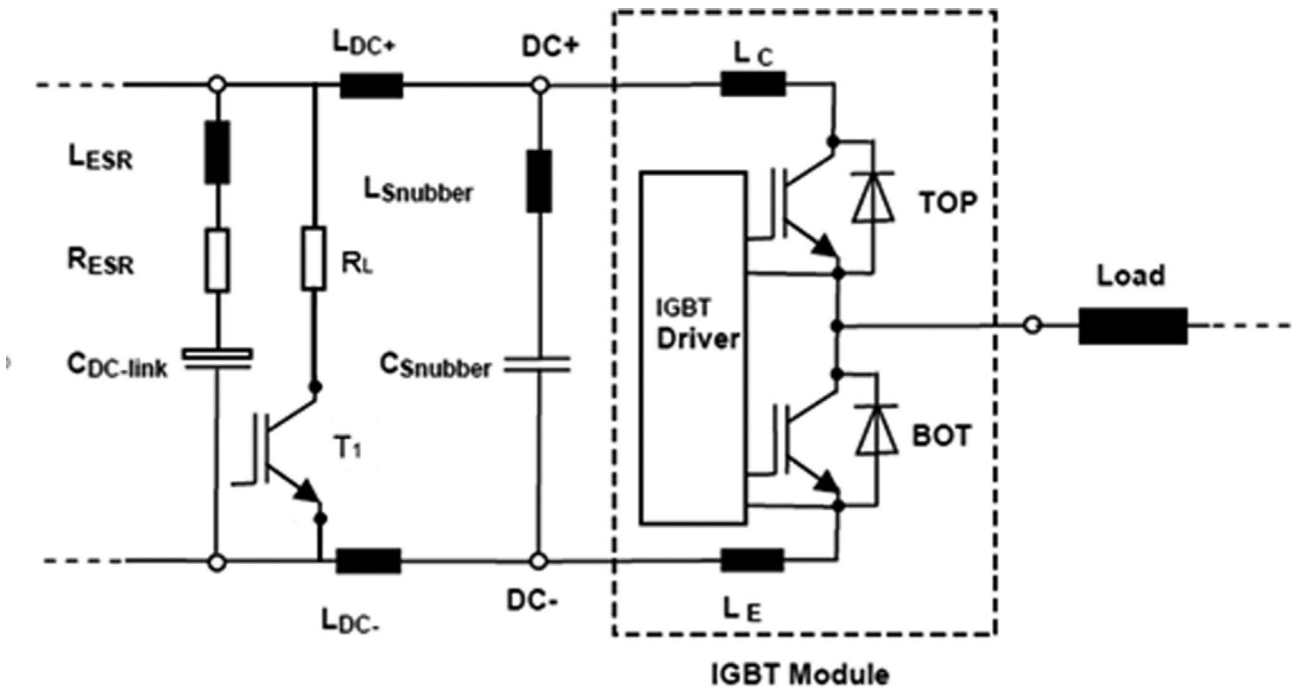
Figure 31. Connection diagram of DC-Bus and suppression capacity to power semiconductor (IGBT).

Table 9. Symbols used and their explanations.

Symbol	Description
$C_{da\text{-}link}$	DC-bus Capacitance value
$C_{Snubber}$	Snubber Capacitance value
L_{ESR}	DC-bus Capacitance series equivalent inductance
R_{ESR}	DC-Bus Capacitance series equivalent resistance
L_c	Parasitic inductance of the collector
L_E	Parasitic inductance of the emitter
$L_{DA+}, L_{DA\text{-}}$	Bus-bar interference inductances
R_L	Load Resistant
T_1	Power Semiconductor (IGBT)

during switching. These snubber capacitances are used as a low-pass filter in a sense. In the system installation, it is mounted adjacent to the DC-bus terminals of each power semiconductor module in order not to increase the stray inductance value. Correctly calculated R_{on} and R_{off} resistors should be used in the design of the power semiconductor driver circuit. These resistors affect the conduction and cut-off time of the power semiconductor, that is, its fast switching on and off. It is very important to keep the BOTtom power semiconductor in cutoff while the TOP power semiconductor of the power semiconductor driver is in conduction. In the power semiconductor driver design,

a design should be made to keep the gate voltage of the Bot Switching semiconductor at -7V and to prevent the power semiconductor from conducting in the opposite direction. It is very important to develop the control software in such a way that it will stop the entire system in case of voltage cuts and overheating of the system shown in figure 32. The electrical isolation of the control stage and the power stage is of great importance for safety. For this reason, opto-coupler in accordance with automotive standards should be used to provide isolation between the control stage and the power stage and to transmit control signals optically. It is important to measure the system temperature values and the current of each phase and DC-Bus. It is very important to monitor the temperature, current and voltages in the control software, to run the interrupt structure of the microcontroller with a fault message in case of exceeding the limits, and to stop the system. So the system can be protected. The source of the errors that will cause the interrupt; excessive current draw, simultaneous transmission of TOP and BOTTOM semiconductors, not using die band, and overheating of the circuit. The explanations of the symbols used in the circuit diagram shown in Figure 31 are shown in Table 9. In all these cases, the system must be stopped immediately for protection. In case the DC-Bus voltage exceeds the nominal value, DC-Bus capacitor should be used as seen in figure 31 to take this voltage and ensure safety. Sandwich DC-bus design is an important factor to reduce stray inductance. Appropriate cooler selection should be made in the power floor and attention should be
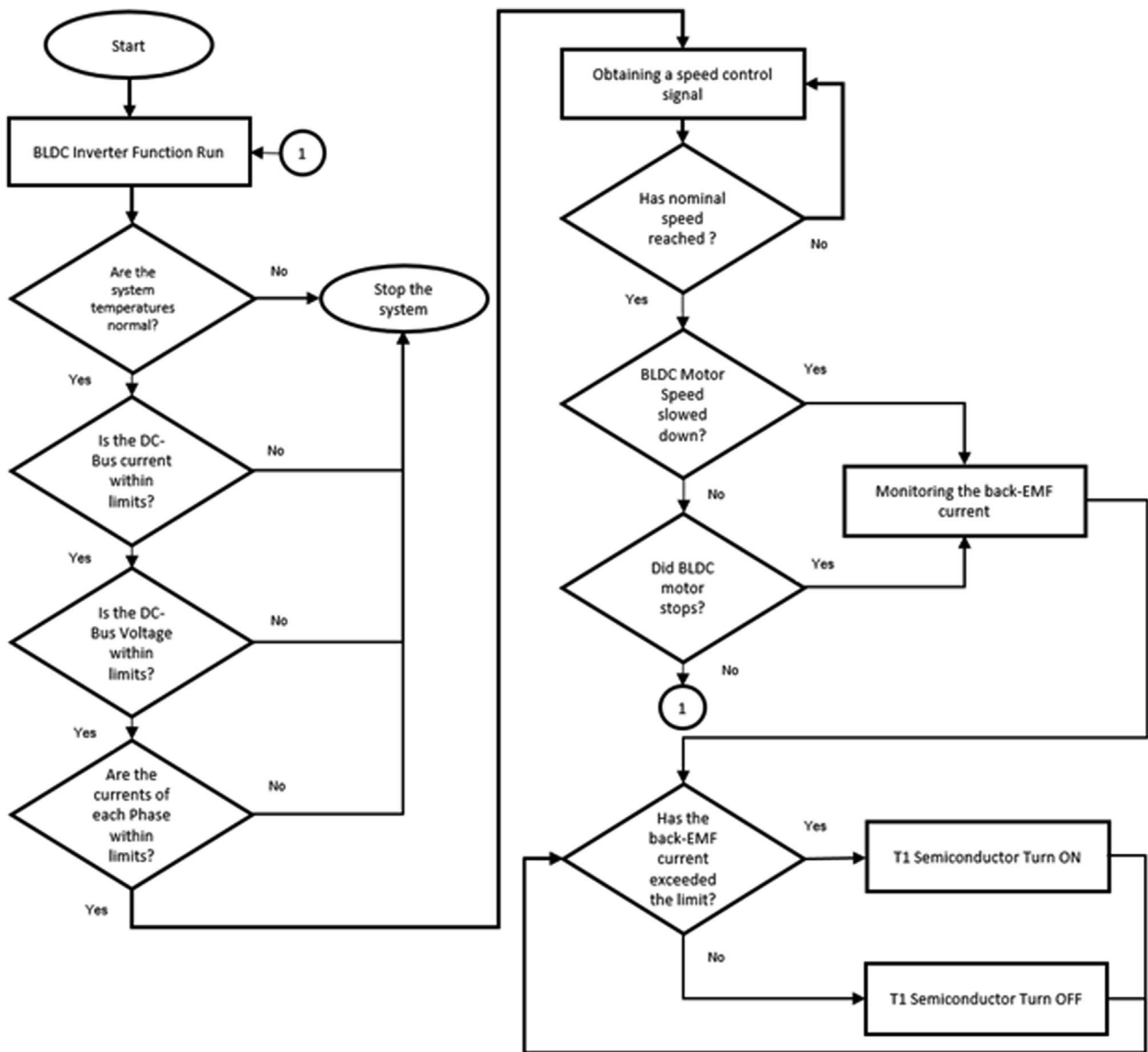
Figure 32. Flow chart of the proposed algorithm to be added to the control algorithms developed in high-power systems for safe and efficient operation.

paid to the placement of the power semiconductors. The flow diagram of the proposed algorithm to be added to the control algorithms developed in high-power systems for safe and efficient operation is shown in Figure 32. It is recommended to add the algorithm in the flow diagram shown in figure 32 to all control software developed to operate at high power. This is important in terms of system efficiency and safety, as system temperatures, DC-link current and voltage, phase currents, motor speed, torque, deceleration and stopping of the motor are monitored. All these measures have been carried out in this study and the developed

algorithms have been ensured to work safely and stably in high-power systems.

CONCLUSIONS

In this study, the basic parameters for a passenger electric vehicle were determined, a simulation model of the vehicle was obtained and using this obtained model, the appropriate electric motor was selected. Later on, an original 75 kW DC-AC Converter (Inverter) in accordance with automotive standards was designed for the Brushless DC

motor used for vehicle drive and was successfully used for tests in practice.

Simulation and experimental results demonstrated the effectiveness of the originally developed drive system. It has been shown that a fuzzy controller successfully controls the BLDC motor and the model-based programming of dSPACE, is very simple and versatile when comparing to traditional methods. It has been observed that the proposed fuzzy logic controller performs better than the PID technique. Experimental results show that the proposed fuzzy logic control method better compensates for the effects of time-varying load, while reducing steady-state error more than other methods as time progresses. The performance and accuracy of the algorithms have been tested in practice and the BLDC motor phase currents and voltages have been monitored with an oscilloscope. The simulation results and the application results have been consistent with each other, and the system performance has been successfully tested. Problems caused by high power operation have been resolved. In order to ensure that the control algorithms work effectively and safely at high power, the necessary solutions have been specified and successfully implemented.

AUTHORSHIP CONTRIBUTIONS

Authors equally contributed to this work.

DATA AVAILABILITY STATEMENT

The authors confirm that the data that supports the findings of this study are available within the article. Raw data that support the finding of this study are available from the corresponding author, upon reasonable request.

CONFLICT OF INTEREST

The author declared no potential conflicts of interest with respect to the research, authorship, and/or publication of this article.

ETHICS

There are no ethical issues with the publication of this manuscript.

REFERENCES

[1] Tutelea L, Boldea I. Optimal design of residential brushless d.c. permanent magnet motors with FEM validation. 2007 International Aegean Conference on Electrical Machines and Power Electronics Electromotion (ACEMP'07); 2007 Sept 10-12; Bodrum Turkey: IEEE; 2007. pp. 435–439. [CrossRef]

[2] Zarko D, Ban D, Lipo TA. Analytical solution for cogging torque in surface permanent-magnet motors using conformal mapping. IEEE Trans Magn 2007;44:52–64. [CrossRef]

[3] Ustun O, Yilmaz M, Gokce C, Karakaya U, Tuncay RN. Energy management method for solar race car design and application. IEEE International Electric Machines and Drives Conference; 2009 May 03-06; Miami, FL: IEEE; 2009. pp. 804–811. [CrossRef]

[4] Markovic M, Hodder A, Perriard Y. An analytical determination of the torque–speed and efficiency– speed characteristics of a BLDC motor. Energy Conversion Congress and Exposition; 2009 Sept 20-24; San Jose, CA: IEEE; 2009. pp. 168–172. [CrossRef]

[5] Zhao L, Ham C, Zheng L, Wu T, Sundaram K, Kapat J, et al. A highly efficient 200000 rpm permanent magnet motor system. IEEE Trans Magn 2007;43:2528–2530. [CrossRef]

[6] Tuncay RN, Ustun O, Yılmaz M, Gokce C. Karakaya U. Design and implementation of an electric drive system for in-wheel motor electric vehicle applications. 7th IEEE Vehicle Power and Propulsion Conference; 2011 Sept 06-09; Chicago, IL: IEEE; 2011. pp. 1–6. [CrossRef]

[7] Nair SS, Nalakath S, Dhinagar SJ. Design and analysis of axial flux permanent magnet BLDC motor for automotive applications. IEEE International Electric Machines & Drives Conference (IEMDC'11); 2011 May 15-18; Niagara Falls, Canada: IEEE; 2011. pp. 1615–1618. [CrossRef]

[8] Park SJ, Park HW, Lee MH, Harashima F. A new approach for minimum-torque-ripple maximum-efficiency control of BLDC motor. IEEE Trans Ind Electron 2000;47:109–114. [CrossRef]

[9] Zarko D, Ban D, Lipo TA. Analytical calculation of magnetic field distribution in the slotted air gap of a surface permanent-magnet motor using complex relative air-gap permeance. IEEE Trans Magn 2006;42:1828–1837.

[10] Rahim NA, Ping HW, Tadjuddin M. Design of axial flux permanent magnet brushless DC motor for direct drive of electric vehicle. IEEE Power Engineering Society General Meeting; 2007 Jun 24-28; Tampa, USA: IEEE; 2007. 10290216. [CrossRef]

[11] Soong WL, Miller TJE. Field-weakening performance of brushless synchronous AC motor drives. IEE Proc Electr Power Appl 1994;141:331–340. [CrossRef]

[12] Wu B. Brushless DC Motor Speed Control. Master Thesis. Dep of Electrical & Computing Engineering, Ryerson University, October, 2001.

[13] Premkumar K, Manikandan BV. Bat algorithm optimized fuzzy PD based speed controller for brushless direct current motor. Eng Sci Technol Int J 2016;19:818–840. [CrossRef]

[14] Chico A, Brillianto H, Maghfiroh H. Fuzzy logic controller and its application in brushless DC motor

(BLDC) in electric vehicle. J Electrical Electronic Inform Commun Technol 2021;3:35−43. [CrossRef]

[15] Agrawal S, Vivek S. Particle swarm optimization of BLDC motor with fuzzy logic controller for speed improvement. 2017 8th International Conference on Computing, Communication and Networking Technologies; 2017 Jul 3-5; Delhi, India: IEEE; 2017. 17418417. [CrossRef]

[16] Wang H, Li P, Shu Y, Kang D. Double closed loop control for BLDC based on whole fuzzy controllers. 2nd IEEE International Conference on Computational Intelligence and Applications; 2017 Sept 08-11; Beijing, China: IEEE; 2017. 17415277. [CrossRef]

[17] Davoudkhani IF, Akbari M. Adaptive speed control of brushless DC (BLDC) motor based on interval type-2 logic. 24th Iranian Conference on Electrical Engineering (ICEE); 2016 May 10-12; Shiraz, Iran: IEEE; 2016. 16375523. [CrossRef]

[18] Wang ZS, Liu CY, Song XL, Song ZY, Yang ZK. Improved variable universe fuzzy PID application in brushless DC motor speed regulation system. Proceedings of the 2016 International Conference on Machine Learning and Cybernetics; 2016 Jul 10-13; Jeju, South Korea: IEEE; 2016. 16692057. [CrossRef]

[19] Hanselman DC. Brushless permanent magnet motor design. 1st ed. New York: McGraw Hill; 1994.

[20] Kenjo T, Nagomori S. Permanent Magnet and Brushless DC Motors. 1st ed. Oxford: Oxford University Press; 1985

[21] Indra F, Era P, Novie AW. Fuzzy gain scheduling of PID (FGSPID) for speed control three phase induction motor based on indirect field oriented control (IFOC). EMITTER Int J Eng Technol 2016;4:237−258. [CrossRef]

[22] Aydogdu O, Levent ML. Trajectory control of a variable loaded servo system by using fuzzy iterative learning PID control. Int J Robot Control Syst 2017;2:170−177.

[23] Xu C, Huang D, Huang Y, Gong S. Digital PID controller for brushless DC motor based on AVR microcontroller. 2008 IEEE International Conference on Mechatronics and Automation; 2008 Aug 05-08; Takamatsu: IEEE; 2008. pp. 247−252.

[24] Tzafestas S, Papanikolopulos NP. Incremental fuzzy expert PID control. IEEE Trans Ind Electron 1990;37:365−371. [CrossRef]

[25] Bahadır A. Brushless direct current motor driver design and adaptive control for electric vehicles. Doctoral Thesis. Konya, Turkey: Konya Technical University; 2021.

[26] Jaya A, Purwanto E, Fauziah MB, Murdianto FD, Prabowo G, Rusli MR. Design of PID-fuzzy for speed control of brushless DC motor in dynamic electric vehicle to improve steady-state performance. 2017 International Electronics Symposium on Engineering Technology and Applications (IES-ETA); 2017 Sept 26-27; Surabaya, Indonesia: IEEE; 2017. 17453328. [CrossRef]

[27] Aziza Z. ANN-Based Current Controlled BLDC Servo-Motor. 9th European Conference on Power Electronics and Applications, EPE 2001, Graz, 27-29 August, 2001.

[28] Bojadziev G, Bojadziev M. Fuzzy Sets, Fuzzy Logic, Applications. River Edge: Word Scientific Publishing; 2000.

[29] Vas Peter. Artificial-Intelligence-Based Electrical Machines and Drives. 1st ed. New York: Oxford University Press; 1999.

[27] Apribowo CHB, Maghfiroh H, Ahmad M. Fuzzy logic controller and its application in brushless DC motor (BLDC) in electric vehicle-a review. Int Conf Electr Eng Inform Commun Technol 2021;3:35−43.

[28] Agrawal S, Vivek S. Particle swarm optimization of BLDC motor with fuzzy logic controller for speed improvement. 2017 8th International Conference on Computing, Communication and Networking Technologies; 2017 Jul 3-5; Delhi, India: IEEE; 2017. 17418417.

[29] Wang H, Li P, Shu Y, Kang D. Double closed loop control for BLDC based on whole fuzzy controllers. 2nd IEEE International Conference on Computational Intelligence and Applications; 2017 Sept 08-11; Beijing, China: IEEE; 2017. 17415277.

[27] Davoudkhani IF, Akbari M. Adaptive speed control of brushless DC (BLDC) motor based on interval type-2 logic. 24th Iranian Conference on Electrical Engineering (ICEE); 2016 May 10-12; Shiraz, Iran: IEEE; 2016. 16375523.

[28] Wang ZS, Liu CY, Song XL, Song ZY, Yang ZK. Improved variable universe fuzzy PID application in brushless DC motor speed regulation system. Proceedings of the 2016 International Conference on Machine Learning and Cybernetics; 2016 Jul 10-13; Jeju, South Korea: IEEE; 2016. 16692057.

[29] Indra F, Era P, Novie AW. Fuzzy gain scheduling of PID (FGSPID) for speed control three phase induction motor based on indirect field oriented control (IFOC). EMITTER Int J Eng Technol 2016;4:237−258.